Available online at www.sciencedirect.com
ScienceDirect
Optics Communications 281 (2008) 401–407
OPTICS COMMUNICATIONS
www.elsevier.com/locate/optcom

Different field distributions obtained with an axicon and an amplitude mask

Marcelino Anguiano-Morales [a,*], Amalia Martínez [a], M. David Iturbe-Castillo [b], Sabino Chávez-Cerda [b]

[a] Centro de Investigaciones en Óptica, C.P. 37150 León, Gto., Mexico
[b] Instituto Nacional de Astrofísica, Óptica y Electrónica, C.P. 72000 Puebla, Pue., Mexico

Received 13 May 2007; received in revised form 18 September 2007; accepted 3 October 2007

Abstract

A combination of an axicon and an amplitude mask is used to obtain an intensity distribution that differs from the typical Bessel one. Experimental and numerical characterization of the field is made for different propagation distances and types of amplitude masks.

PACS: 42.60.Jf; 42.25.Fx; 42.25.Bs; 42.25.Gy

Keywords: Bessel beam; Wave propagation

1. Introduction

Axicon is an optical element that produces a line focus from an incident uniform monochromatic beam. It was introduced by Mcleod in 1954 [1] and since then it has been used in many applications, including alignment, optical tweezers, optical coherence tomography, medical imaging and industry [2–7].

Nowadays, several types of axicons have been proposed (Fresnel axicon, conical mirror, diffractive circular gratings, doublet lenses). When an axicon is illuminated by a uniform plane wave it produces a Bessel intensity distribution. Different type of distributions have been obtained when the incident beam is not uniform, for example, under illumination of a Gaussian or Laguerre–Gaussian beam a Bessel–Gauss or Bessel beam of high order is obtained, respectively.

The aim of this paper is to demonstrate that a combination of an axicon and an amplitude mask with simple transmittance function can produce field distributions that differ from the Bessel and in some cases can keep the characteristic of propagation invariant.

The paper is structured as follows: In Section 2 we describe the characteristics of the axicon and amplitude mask used in the experiments. In Section 3 we describe the experimental results obtained with the different mask and its transversal and on-axis intensity distribution obtained at different distances. A numerical simulation of the experimental conditions is presented in Section 4. Finally, the conclusions are given in Section 5.

2. Axicon, mask and experimental configuration

Experimentally we used an axicon with the following characteristics: a diameter of 2.5 cm with an angle $\gamma = 0.5° = 8.7 \times 10^{-3}$ rad and refractive index $n = 1.5$. When the axicon is illuminated with a uniform monochromatic beam at $\lambda = 633$ nm a Bessel beam is obtained with a distance of invariance, z_{max}, of around 2.6 m. The number

* Corresponding author. Tel.: +52 4774414200; fax: +52 4774414209.
E-mail addresses: anguiano@cio.mx (M. Anguiano-Morales), diturbe@inaoep.mx (M. David Iturbe-Castillo), sabino@inaoep.mx (S. Chávez-Cerda).

0030-4018/$ - see front matter © 2007 Published by Elsevier B.V.
doi:10.1016/j.optcom.2007.10.013

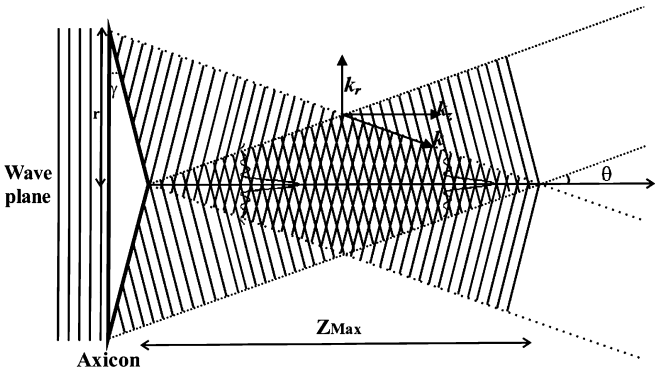

Fig. 1. Side view of the generation of a Bessel beam by means of an axicon. A wave plane is incident on a conical lens, known as an axicon, the additional focusing effect of the axicon causes strong near field interference effects in the region where the deflected beam overlaps with itself. Since, in the geometrical optics limit, the angles of overlap remain constant with the propagation distance, the profile of the interference pattern generated remains essentially invariant over the overlap region.

of observed rings increased as a function of the distance of observation from the axicon, reaching a maximum at a distance of around 1.3 m and after this point decreased. The Bessel distribution does not exist in the whole illuminated area but only in a spatially limited one. This region is formed by a superposition of inward and outward conical Hankel waves, the conical wave generated by the axicon propagates converging and emerging from the optical axis, and the maximum region of interference where conical waves superpose is $z_{max}/2$, as depicted in Fig. 1. The radial spatial frequency, k_r, of the Bessel function is given by $k\sin(n-1)\gamma$, and $k_z = k\cos\theta$ the longitudinal spatial frequencies where k is the wave number. This means that the radial separation of the Bessel rings is dependent not on the diameter of the axicon but only on its apex angle. The extension of the resulting interference zone can be estimated by

$$z_{\max} = \frac{r}{\tan\theta}, \tag{1}$$

where r denotes the nominal radius of the beam, and Snell's law gives the refracted angle $\theta = \gamma(n-1)$ for small angles. In order to have sufficiently extended interference zone for the investigations, a very small angle is preferable. The experimental cross-section intensity distribution obtained at a distance of 100 cm is shown in Fig. 2a. The beam behaves as propagation invariant within a distance of around 1.5 m. After this distance an increase in the on-axis intensity is observed probably due to the edge waves, see Fig. 2b.

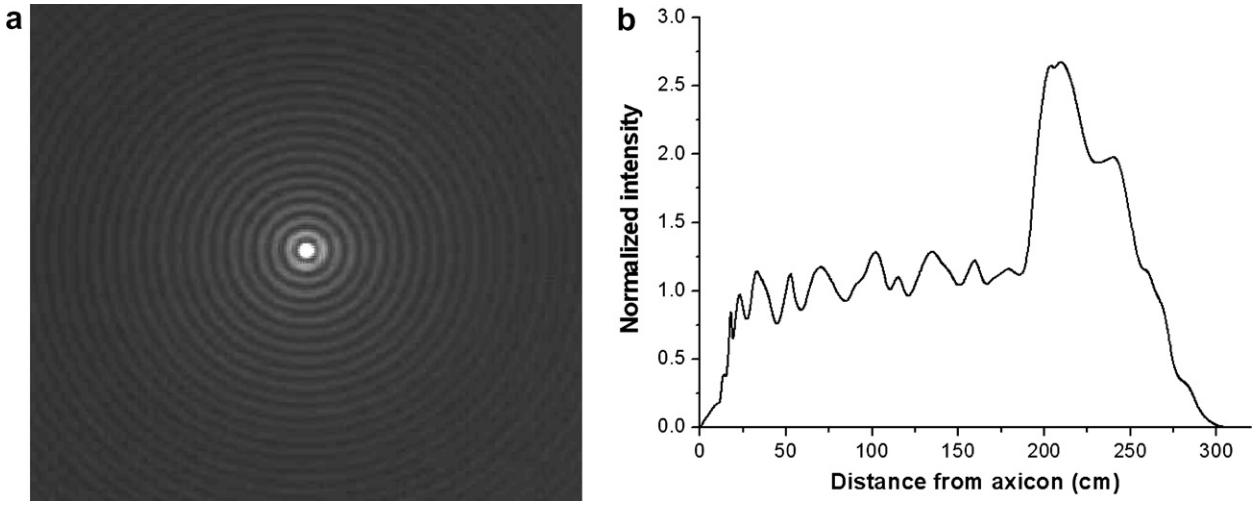

Fig. 2. (a) Typical intensity distribution obtained with an axicon within the longitudinal range and (b) on-axis intensity versus distance z produced in coherent light by an axicon of radius 25 mm, and open angle $\gamma = 0.5^{\circ}$.

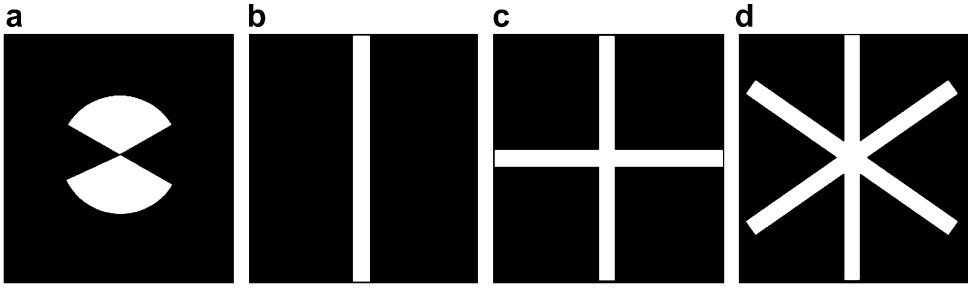

Fig. 3. Schematic diagrams of the different initial conditions that arrive to the axicon.

Amplitude masks of multiple transmittances were fabricated on photographic film; Masks of the type of a single slit and circular sectors of different angular sizes were fabricated, also crossed slits or opaque stripes were used. In Fig. 3 we present the type of mask used in the experiments of the following section. Far-field diffraction patterns of different kinds of apertures have been studied before [8–11], the characteristics of the diffraction patterns of the mask used are remarkably different to those obtained using the combination mask-axicon.

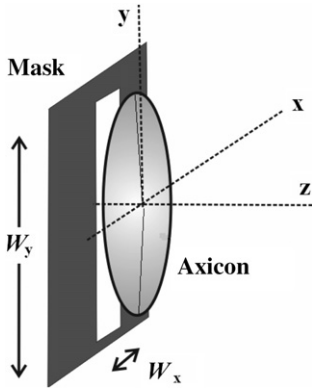

Fig. 4. Diffractive aperture placed immediately in back of axicon.

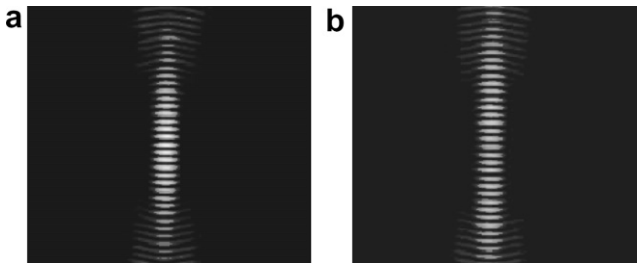

Fig. 5. Distributions obtained using a mask with a single slit of 3 mm at distances of (a) 90 cm and (b) 150 cm from the axicon.

Experimentally, expanded and collimate laser beam from a 30 mW He–Ne laser at $\lambda = 633$ nm was used. The amplitude mask was set close to the axicon to diminish the diffraction effects, see Fig. 4. The intensity distributions at different distances from the mask-axicon combination

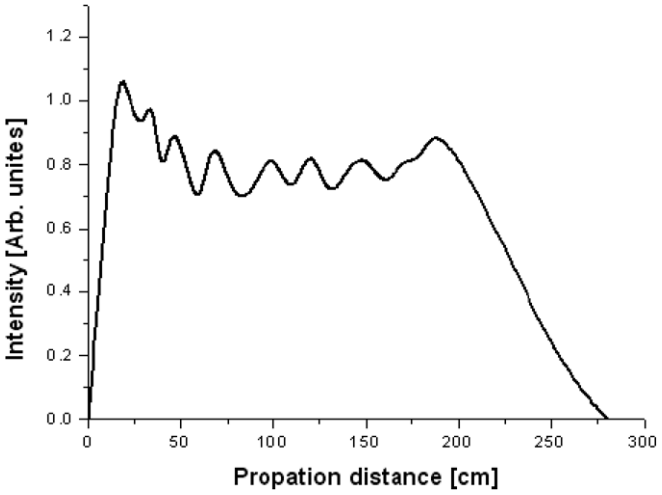

Fig. 7. Intensity on-axis with a single slit of 3 mm.

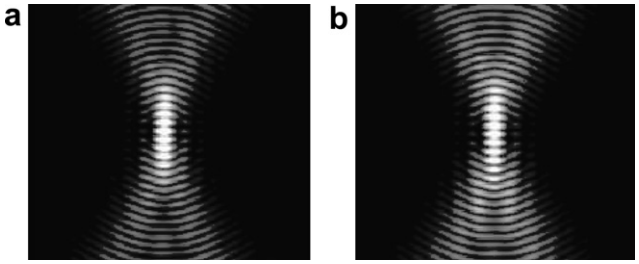

Fig. 8. Distributions generated with a mask with two circular sectors of angle of 70°. Transverse distribution at propagate distance of (a) 90 cm and (b) 150 cm.

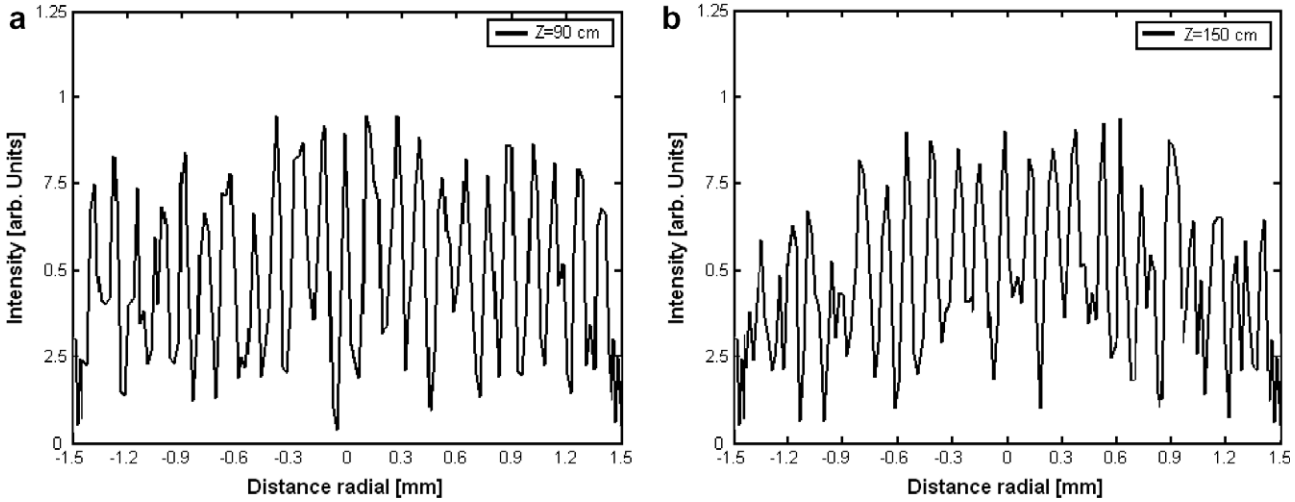

Fig. 6. Profile of intensity of the distributions generated with a single slit of 3 mm at distances of (a) 90 cm and (b) 150 cm.

were obtained with a CCD camera connected to a personal computer.

3. Results

When a mask with a rectangular aperture of 3 mm of width (W_x) and an axicon are illuminated with a plane wave, the resulting intensity distribution was similar to an interference patter with a period of 90 μm. In this case, the obtained distribution did not present a single maximum at the centre, as in the case of a Bessel beam. The transverse distribution recorded at different distances from the axicon, see Fig. 5, did not present notorious changes. The intensity profiles of the distributions shown in Fig. 5 are presented in Fig. 6. We can observe that the maximums of the pattern practically had the same intensity when the distance was 90 cm; however, a decrease was observed for the far-off lobs when the distance was increased. This effect can be due to the influence of the decrease in the conic volume on the region beyond $Z_{max}/2$ (see the schematic representation of Fig. 1).

The on-axis intensity obtained for this configuration is shown in Fig. 7: we can observe that close to the axicon a maximum intensity was obtained, after this distance began to decrease, reaching an oscillatory behaviour for a distance of 50 cm. After a distance of 200 cm the intensity began to decrease reaching a minimum at approximately 280 cm from axicon.

When the incident field was modulated by a mask with two circular sectors of 70°, the generated intensity distributions for different distances, see Fig. 8, presented very similar characteristics to those of the Mathieu beam (fundamental non-diffracting solution of the wave equation in elliptic cylindrical coordinate [12]) along the vertical axis; however in the horizontal direction the distribution was almost Gaussian. The intensity profiles of the distributions shown in Fig. 8 are presented in Fig. 9. The on-axis intensity presents a very smooth behaviour for almost 2 m, see Fig. 10. We think that with this combination it is possible to generate a field distribution that is closer to the propagation invariant Mathieu beam.

When a mask with two orthogonal rectangular slits was used, the generated distribution presented a region where a set of circular spot were arranged in a rectangular array.

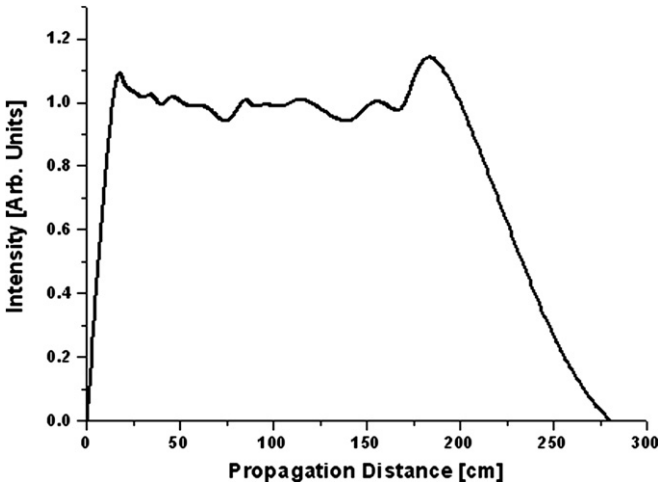

Fig. 10. On-axis intensity, obtained with a mask of two circular sectors of angle of 70°.

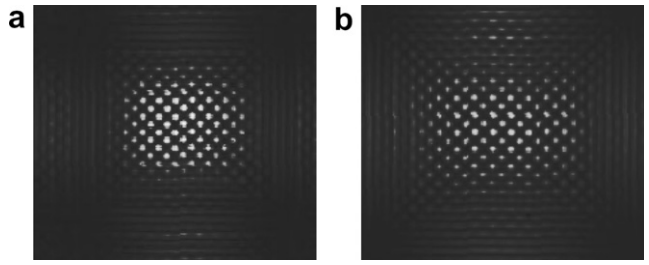

Fig. 11. Distributions obtained using two slits. Intensity distributions obtained at distances of 90 cm and 150 cm from the axicon.

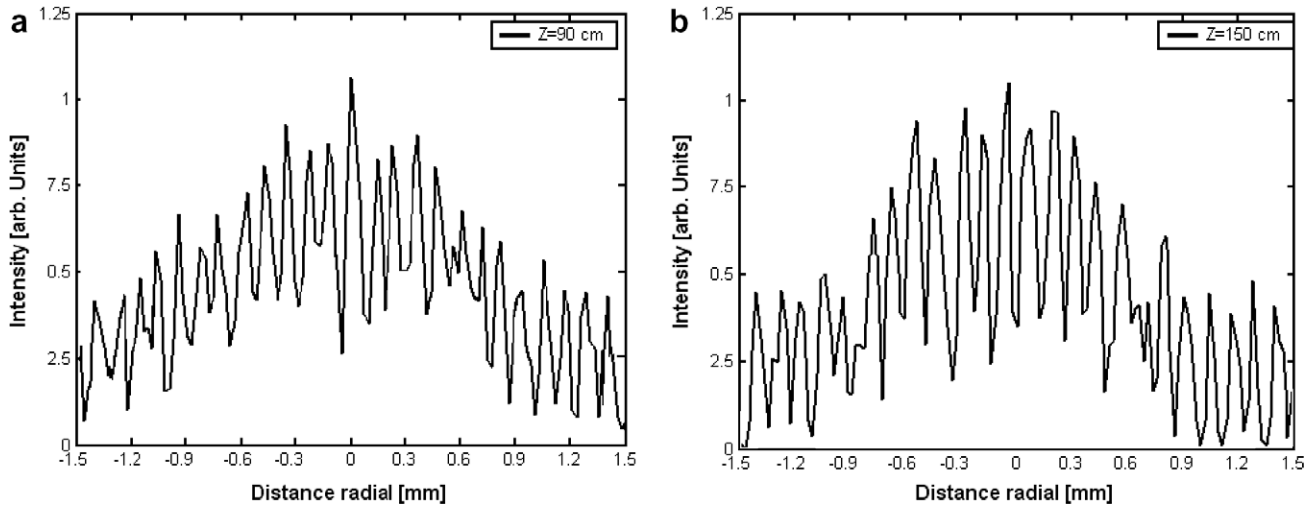

Fig. 9. Intensity profiles at the same distance of the distributions shown in Fig. 6.

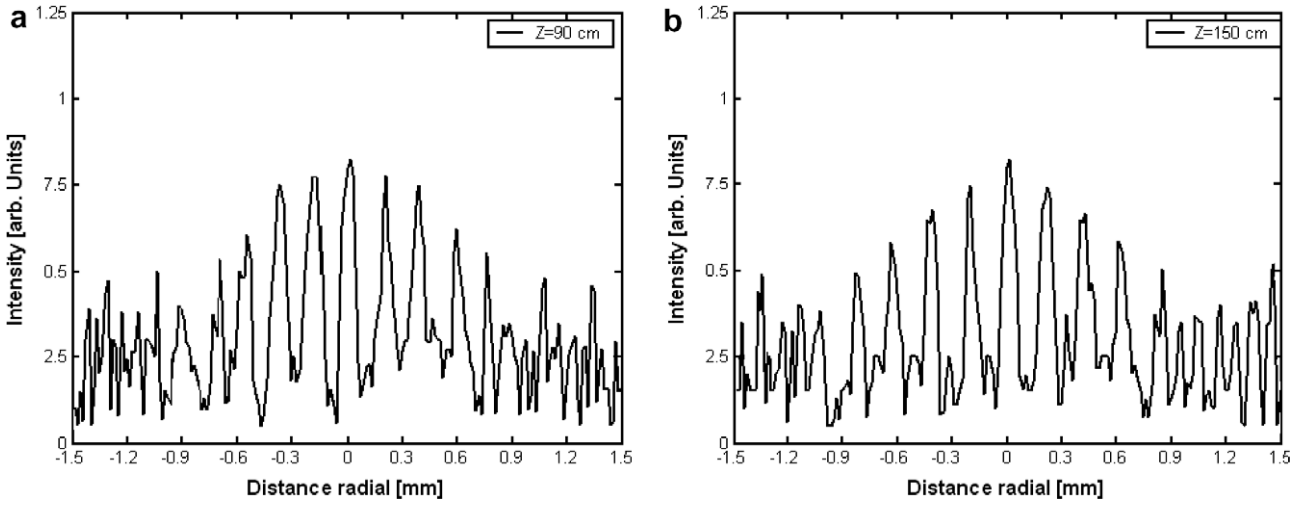

Fig. 12. Intensity profiles at the same distance of the distributions shown in Fig. 8.

The pattern, shown in Fig. 11, presents a distribution similar to the structures of a photonic lattice arranged triangularly. The diameter of the bright spots was of 110 μm, with a separation from centre to centre of 240 μm. The central bright spots present a higher intensity than the others; considerable differences do not exist in both distributions (see Fig. 12). The on-axis intensity presents a very smooth behaviour beyond 50 cm and the oscillations are around 0.85 arbitrary units; this is shown in Fig. 13.

The use of a mask with three rectangular slits generates a hexagonal array of spots. In Fig. 14, the transverse distribution is shown, for two different distances from the axicon. The intensity profile of the distribution detected at 90 cm and 150 cm is shown in Fig. 15. We can observe that maximums of the pattern practically presented the same intensity and that when the distance increased, a decrease was observed for the far-off lobs, as can be seen in Fig. 16. The diameter of the bright spots was about 110 μm. The on-axis intensity presents behaviour without abrupt oscillations. We can observe that the magnitude diminishes initially, but beyond 30 cm, it reaches an almost constant behaviour.

It was interesting to analyze what happens when opaque obstructions were used. The modulation of the incident field with crossed opaque obstructions produced a dark hole in the centre of the distribution. When a beam was obstructed by 18 opaque rectangular obstructions, the intensity was initially null in the central part. After propagation, the central part of the distribution took a structure that obeys a Bessel function, while on the outer region of such central part there are discontinuous circular fringes; this type of distributions had been proposed numerically with the name of kaleidoscopic [13]. It is interesting to note that does not matter that the mask affects the cross-section of the incident distribution to the axicon hence a Bessel beam is reconstructed in the central part, see intensity profile in Fig. 17c, This result confirms that the reconstruction of a Bessel beam is due to the conical waves that the axicon produce. Special attention is made in the case of a circular sector because we think that it produces propagation invariant beams. For example, in the case of an angular sector of 70° we obtain the following intensity cross-section for different propagation distances, and the on-axis intensity followed a very constant behaviour, see Fig. 10 when the angle was reduced the intensity distribution was changed, but the on-axis intensity distribution followed the

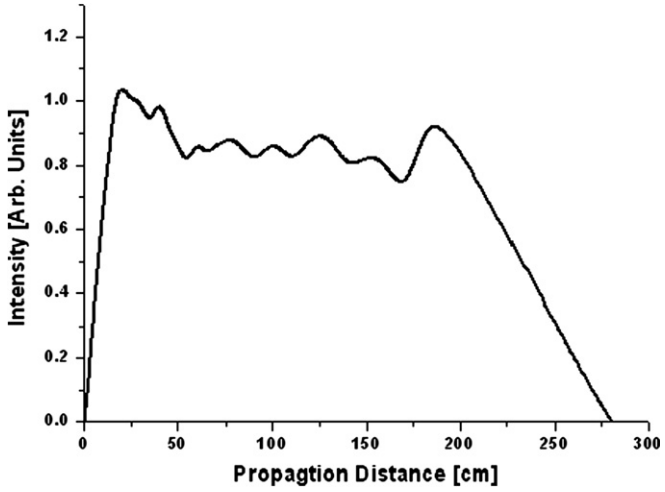

Fig. 13. Intensity on-axis generated with two slits.

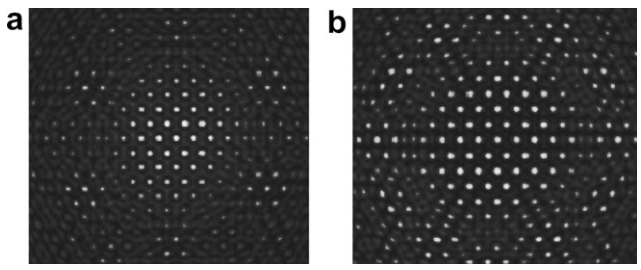

Fig. 14. Distributions obtained using three slits. Intensity distributions obtained at distances of 90 cm and 150 cm from the axicon.

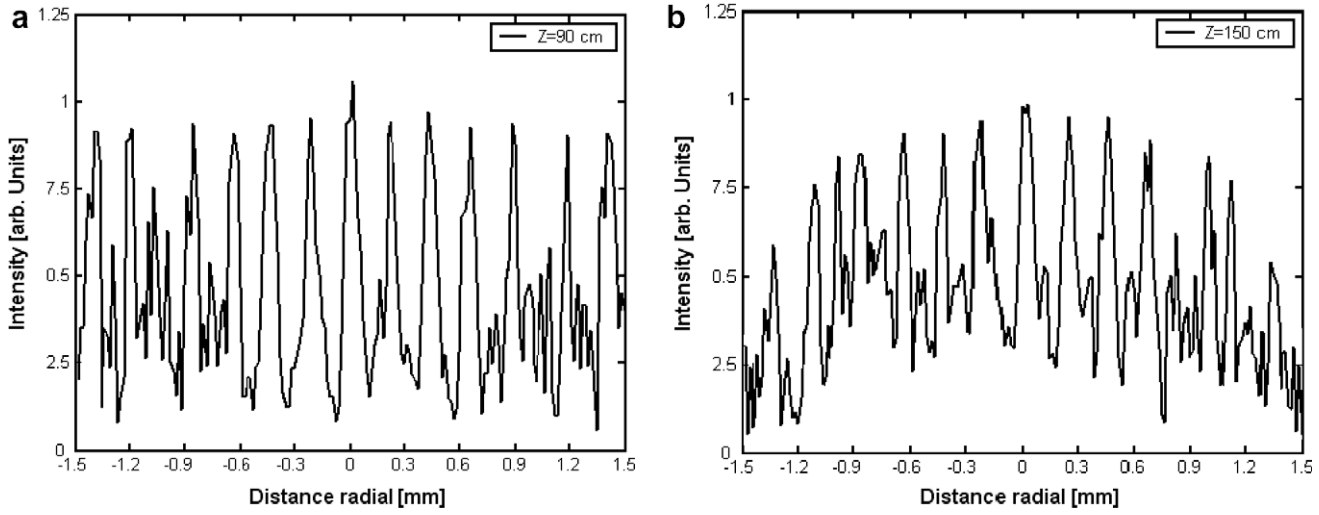

Fig. 15. Intensity profile at the same distances that the distributions shown in Fig. 13.

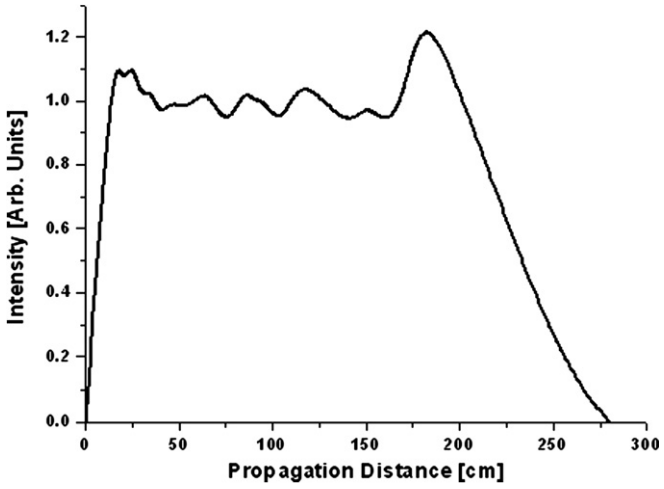

Fig. 16. Intensity on-axis generated by means of three slits crossed at an angle 60°.

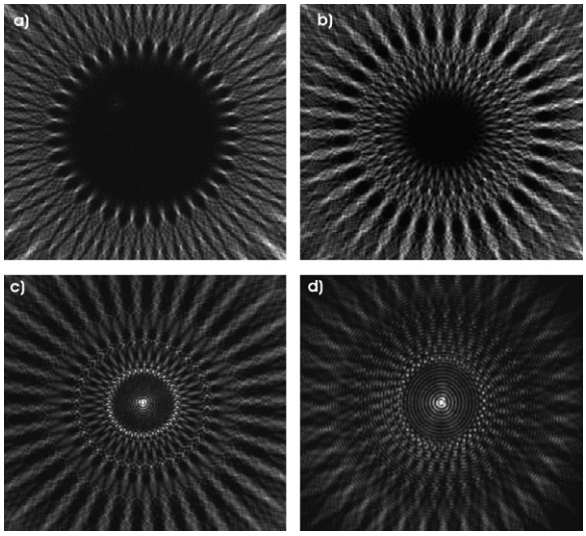

Fig. 17. Distribution obtained using a mask with 18 crossed opaque obstructions with width of 0.3 mm the pattern is registered at a distance of (a) 13 cm, (b) 31 cm, (c) 51 cm, and (d) 121 cm from the axicon.

same behaviour that in the previous case. This results in very good agreement with the reported in [12].

4. Numerical simulations

The propagation of the beam was obtained using the split-step beam propagation method. We used a Hankel function $H_0^{(2)}(k_r r)$, that represents a zero-order Hanke function of second type, to describe the influence of the axicon [13]. The incident optical field modulated by the mask was considered by the function $A(x,y)$. Then, the field $U(x,y)$ just after the axicon was the product of $A(x,y)$ with $H_0^{(2)}(k_r r)$. For example in the case of one rectangular mask we obtain

$$U(x,y) = A(x,y)\left[\mathrm{rec}\left(\frac{x}{W_x}\right)\mathrm{rec}\left(\frac{y}{W_y}\right)\right]H_0^{(2)}(k_r r). \qquad (2)$$

The numerical simulation of the transverse intensity profile of the beam is illustrated in Fig. 18 obtained at distance of 60 cm from the axicon for different masks: (a) a rectangular slit, (b) two orthogonal rectangular slits, (c) three rectangular slits, (d) four, (e) six, and (f) eight crossed apertures. These patterns can also be interpreted as the superposition of N plane waves possessing the same amplitude and phase whose propagation vectors continuously cover the conical surface. Fig. 18a shows the calculated intensity distribution for a rectangular aperture of widths W_x and an axicon. The length W_y was selected to be much larger than W_x. Fig. 18b shows the beam geometry of our simulation of two apertures and an axicon. The two apertures were symmetrically placed around the z axis, and formed an angle of 90° with each other. The interference of those sections of beams resulted in an array of circular spots organized in a Cartesian fashion. Experimentally, this is shown in Fig. 11. One can see that there is a good correspondence between the both. When a mask with three

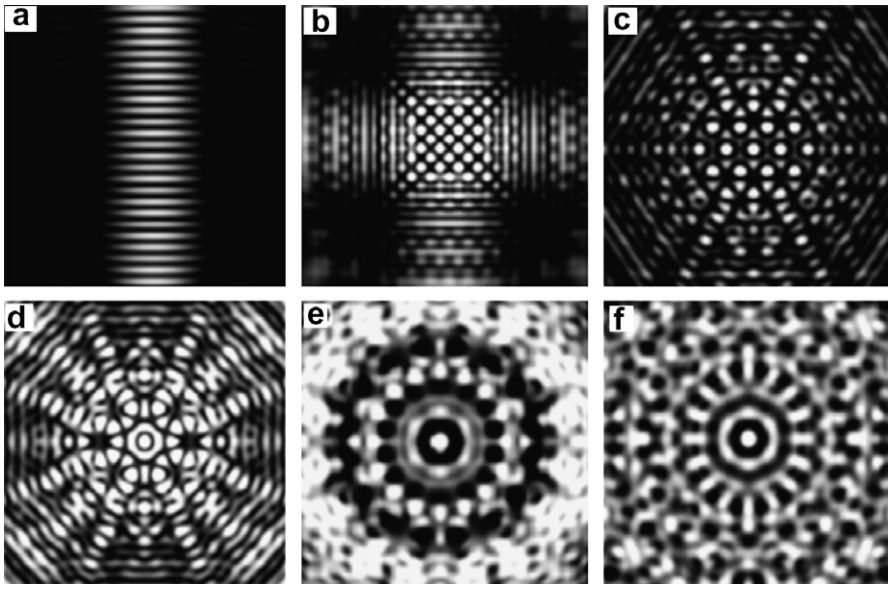

Fig. 18. Distribution obtained numerically using amplitude mask with a (a) one, (b) two, (c) three, (d) four, (e) six, and (f) eight crossed apertures, the distribution is registered at a distance of 60 cm from the axicon.

rectangular slits was used, the obtained distribution presented a region with bright spots in an hexagonal configuration, as it is shown in Fig. 18c.

5. Conclusions

In this work, we demonstrate experimentally and numerically that the intensity distribution obtained with an axicon can differ from the typical Bessel distribution when an amplitude modulation is introduced to the incident beam. Simple masks that consisted of slits or opaque rectangular obstruction allow obtaining patterns that in some cases keep the propagation an invariant property. Possible applications include photonic structures or multiple-beam optical tweezers.

Acknowledgements

The authors wish to thank to Mario Alberto Ruiz for the constructive comments.

References

[1] J.H. McLeod, J. Opt. Soc. Am. 44 (1954) 592.
[2] Zbgniew Jaroszewicz, Ana Burvall, Ari T. Friberg, Opt. Photon. News (2005) 34.
[3] Ming-Dar Wei, Wen-Long Shiao, Yi-Tse Lin, Opt. Commun. 248 (2005) 7.
[4] J. Arlt, K. Dholakia, J. Soneson, E.M. Wright, Phys. Rev. A 63 (2001) 063602-1.
[5] M.R. Wang, C. Yu, Opt. Eng. 40 (2001) 517.
[6] J.A. Davis, E. Carcome, D.M. Cottrell, Appl. Opt. 35 (1996) 599.
[7] Pierre-Andre Belanger, Marc Rioux, Appl. Opt. 17 (1978) 1080.
[8] V.G. Magurin, V.A. Tarlykov, Opt. Spectrosc. 88 (2000) 568.
[9] R.A. Lessard, S.C. Som, Appl. Opt. 11 (1971) 811.
[10] Adolf W. Lohmann, Jorge Ojeda-Castañeda, Alfonso Serrano-Heredia, Appl. Opt. 34 (1995) 317.
[11] Gonzalo Urcid, Alfonso Padilla, Appl. Opt. 44 (2005) 7677.
[12] J.C. Gutierrez-Vega, M.D. Iturbe-Castillo, G.A. Ramirez, E. Tepichin, R.M. Rodriguez-Dagnino, S. Chavez-Cerda, G.H.C. New, Opt. Commun. 195 (2001) 35.
[13] Zdenek Bouchal, Czechoslovak J. Phys. 53 (2003) 537.